GANITA,Vol.74(2), 2024, 429-442

IMPACT OF RICE BRAN BIODIESEL ON THE EFFICIENCY AND ENVIRONMENTAL POLLUTANTS OF ALUMINA NANO ADDITIVES IN COMPRESSION IGNITION ENGINES: A MATHEMATICAL MODEL

ABHIJEET MAURYA ✉, BHANU PRATAP SINGH, AJAY KUMAR SHARMA and RACHANA PATHAK

Abstract

People are quite concerned about the current state of fossil fuel consumption, reduction, and pollution that results from it. In recent times, biodiesel has gained popularity as a fossil fuel substitute. The characteristics of nanoparticles have captivated researchers to employ them as fuel additives in CI engines because of their superior thermophysical and thermochemical capabilities, and biodiesel has greater attributes than diesel fuel. This study compared the usage of B10, B20, and B 30 rice-bran oil biodiesel combined with 90ppmAl_2O_3 nanoparticles with diesel as the base fuel. When using the transesterification procedure, rice-bran BD is prepared, and Al_2O_3 nanoparticles are combined with it using ultrasonication. The effect of the adding nanoparticle in biodiesel on the environment is studied with the aid of thinking about a nonlinear mathematical model. In this paper interaction among Gasses emitted by CI engines, Biodiesel and Nanoparticles is proposed and analysed. The mathematical system is analysed mathematically regarding the nature of equilibrium points and their stability using the theory of nonlinear ordinary differential equations. Numerical simulations illustrate the analytical consequences.

2010 *Mathematics subject classification:* Mathematical Subject Classification: 92B05.

Keywords and phrases: Biodiesel, CI engine, Exhaust Emissions, Nanoparticles, Performance, Mathematical Modelling, Stability.

1. Introduction

The globe is now dealing with several emissions-related problems due to the growing pollution from the automotive sector. Global warming, natural disasters, and health-related problems are emerging because of increased pollution. Furthermore, people's salaries and savings are being impacted by the rising cost of fuel. Consequently, improving engine
performance and lowering related harmful emissions are now urgently needed. It has been discovered that this issue may be resolved by blending biodiesel with nanoparticles to produce nano fuel. In this experimental study, diesel is mixed with 90 PPM of aluminum oxide (Al_2O_3) and rice bran biodiesel to increase engine performance (BTE and BSFC) and improve combustion properties (maximum cylinder

pressure, rate of EGT, and so on). It also reduces emissions (NO_X, carbon monoxide, CO_2, and HC), as well as noise pollution (dBa), all without altering the engines.

Numerous researchers conducted experiments using various nanoparticles. These included non-metal oxides such as graphene oxide (GO) and carbon nanotubes (CNT) in addition to metal oxides such as aluminium oxide (Al_2O_3), copper oxide (CuO), iron oxide (Fe_2O_3), zinc oxide (NO), silicon oxide (SiO_2), and titanium oxide (TiO_2). Regarding engine factors, their findings varied. In order to increase the efficiency and pollutants qualities of fuels that decrease emissions while boosting efficiency, using nanoparticles as an addition to biodiesel has drawn the attention of several researchers in recent years [1-4]. Fuel's thermophysical characteristics improve as a result of nanoparticles. The quantity of nanoparticles in fuel boosts its thermophysical qualities, including heat conductivity and a larger surface to volume ratio. Recently, a range of oxygen impacts on biofuels have been studied to increase the efficiency and emission of internal combustion engines [5,6]. Numerous researchers have conducted experiments to look at how nanoparticles and biodiesel interact in CI engines. Results for ferrocene nanoparticles with biodiesel as well as diesel at 300, 250, 200, 150, 75, and 50 PPM concentrations were examined by Elwardany et al. [8]. A few researchers have also looked at the characteristics of rice bran biodiesel. Acharya et al. [12] investigated two modes of a singlecylinder, four-stroke engine operating at 500 RPM in an experimental investigation on rice bran biodiesel. First, at the preheated stage at 1200C, it revealed reductions in BSFC as well as exhaust pollutants including CO and UBHC [13]. Two further researchers, together with Aalam and Sarvanan [14], examined the effects of Al_2O_3 nanoparticles in combined Mahua oil BD and diesel. In addition to finding a decrease in BSFC, they also observed increases in cylinder pressure, peak pressure, and heat release rates. After adding alumina nanoparticles, the performance was enhanced and emissions including NO_x, CO, and UHBC reduced [15, 16]. The paper is organized as follows: In Section 2, we describe about real world problem with methods. According to section 2, we develop nonlinear mathematical model in section 3 and section 4, analysed mathematical model regard equilibria and their positive conditions. In Section 5, we investigate the stability of positive equilibrium. In Section 6, some numerical
supports are carried out to justify the analytic results obtained in the manuscript and also compare with experimental results. Section 7 deals with the conclusions of the paper.

2. Materials and Methods

The waste (husk) left over after paddy is turned into rice is used to make rice bran oil, an inedible oil. The second-largest rice producing hub is in India. Based on data from the Indian government, 1031 lakh tonnes of rice oil were produced in 2016-2017, and from 2019 to 2020, the amount produced per acre increased significantly. The transesterification process, which is frequently assisted by both homogeneous and heterogeneous catalysts, yields rice bran biodiesel from the reaction. The homogenous

catalyst contains both acids and alkalis [19]. The following reactions are used to produce rice bran oil.

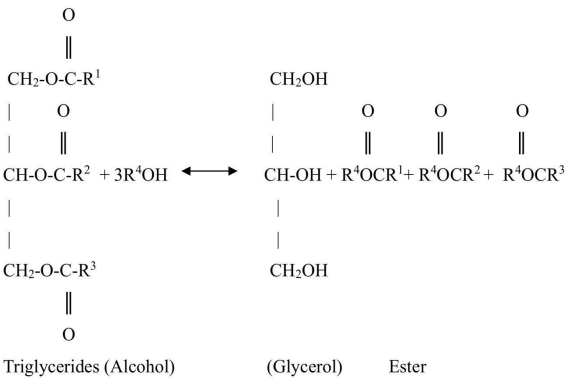

Figure 1 Chemical Reaction in the process of Transesterification method [19].

Nanosized (50 nm) nanoparticles are employed to combine the fuel. As a result, the gasoline and nanoparticles mix more freely and don't become trapped during injection. SEM pictures of aluminium oxide nanoparticles are displayed in Figure 2.

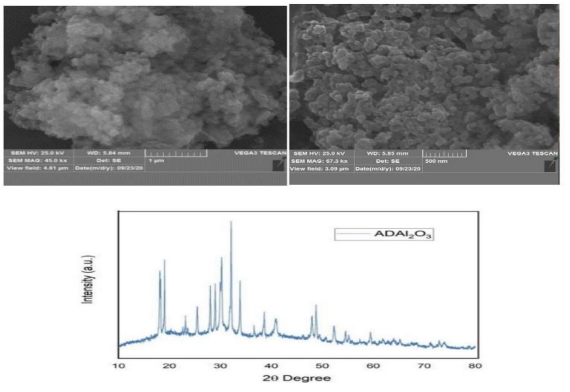

Figure 2 SEM images and Graph for intensity of Al_2O_3.

The procedure of ultrasonication is used to prepare the fuel. For the experiment, three different types of biodiesels-B10, B20, and B30-were employed. 10% rice bran biodiesel is mixed to create B10 biodiesel, 20% rice bran biodiesel is mixed to create B20 biodiesel, and 30% rice bran biodiesel is mixed to create B30 biodiesel, which is made with 70% diesel. Aluminium oxide (Al_2O_3) nanoparticles at a concentration of 90 PPM are introduced to the fuel blend using an ultrasonication procedure after diesel and biodiesel have been combined for up to 1.5 hours using a magnetic stirrer.

The procedure of ultrasonication is used to prepare the fuel. For the experiment, three different types of biodiesels-B10, B20, and B30-were employed. 10% rice bran biodiesel is mixed to create B10 biodiesel, 20% rice bran biodiesel is mixed to create B20 biodiesel, and 30% rice bran biodiesel is mixed to create B30 biodiesel, which is made with 70% diesel. Aluminium oxide (Al_2O_3) nanoparticles at a concentration of 90 PPM are introduced to the fuel blend using an ultrasonication procedure after diesel and biodiesel have been combined for up to 1.5 hours using a magnetic stirrer. Subsequently, the fuel blend is allowed to sit for a full day before being injected into a diesel engine. Table 1 lists the characteristics of nanoparticles, biodiesel, and diesel (base fuel). For this experiment, Ad Nano Technologies Pvt. Ltd. in Karnataka, India, provided the nanoparticles.

Figure 3 magnetic stirrer process for fuel preparation.

Table 1 Properties of materials

Item	Value
Molecular Formula	Al_2O_3
Particle Size	50 nm
Molecular Weight	101.96 g/mol
Bulk Density	0.5 g/cm^3
Melting Point	2055°C
Purity	99.9%

Table 2 Properties of fuel.

Properties/ fuel	D100 (Neat)	B10	B20	B30	RB10Al 30	RB20AI 30	RB30AI 30	Standard
Density, Kg/m^3, 15^{0}C	837	831	835	852	839	857	891	ASTM D-1298
Heating Value (MJ/Kg)	44.0	45.43	45.90	44.05	44.2	45.08	45.03	ASTM D240
Kinematic Viscosity, 40°C	3.8	3.31	3.79	4.9	4.12	4.11	4.03	ASTM 7042

Flash point (**C**)	74	185	188	76	81	83	84	ASTM D-93

An analysis of the CI Engine's performance-

Analysis for BSFC-

This factor gauges a diesel engine's performance by looking at how much fuel it uses specifically. When the engine runs at various loads, it is measured by how much petrol is used in an hour. The BSFC increases at all loads after the nanoparticles are combined; however, when the nanoparticles are blended with plain diesel, the D100A190 fuel consumes the least at a high load (3.5 kW). At 1.5 kW, 2.5 kW, and 3.5 kW , respectively, the greatest boost of 29.84%, 35.2%, and 45% was discovered for RB20A190, RB30A190, and RB20A190. This occurs because the addition of Al_2O_3 nanoparticles increases the amount of oxygen accessible in biodiesel, improving fuel atomization and enabling optimal burning, raising the level of temperature in the fuel's combustion chamber. Heat discharge rates also improve because of this process.

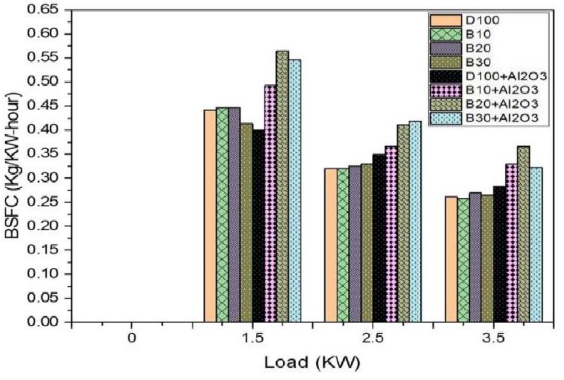

Figure 4 Graph for BSFC versus loads.

Analysis on Exhaust Emissions-

Reducing the engine's significant damaging exhaust emissions is the primary goal of this study.

CO_2 Emissions-

Better fuel atomization, which gives the fuel an excessive quantity of oxygen, causes the CO_2 emissions to rise. As a result, CO is changed into CO_2 [21]. The CO content of nano fuel determines the proportion of CO_2 content. The increase in CO_2 concentration is shown by
the decrease in CO content [13]. Ultimately, the CO_2 concentration is dependent on the air-fuel mixture's equivalency ratio. It is crucial that the mixture be rich in order

to reduce CO_2. In comparison to plain diesel, this experimental investigation revealed an improvement in CO_2 concentration. In the experiment, the greatest decreases for B20 and B10 at 0 kW and 1.5 kW load, respectively, were determined to be 8.6% and 3.84%. For B 10 , the CO_2 emission figure stays the same at 2.5 kW of load.

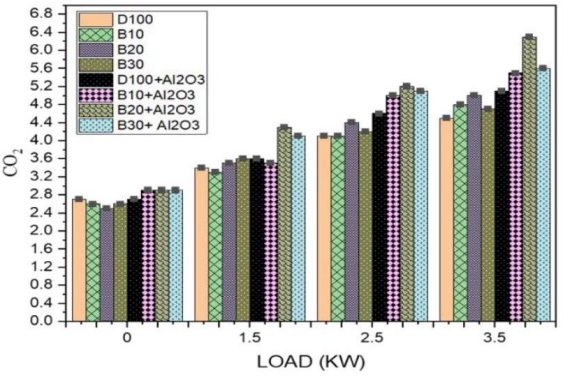

Figure 5 Graph for CO_2 versus Loads

NOx Emissions-

Due to its direct impact on the ozone layer, NO_X is to blame for global warming. The highest reduction of NOx from the exhaust in this experimental investigation is 18.19%. This is a result of the combustion chamber's optimum temperature conditions and an abundance of oxygen. In comparison to neat diesel (D100), the NOX content at $0, 1.5, 2.5$, and $3.5 -$ kW loads decreases by $18.19\%, 13.34\%, 12.20\%$, and 8.79% for RB30Al90, RB10A190, RB30, and RB30, respectively, due to the effect of Al_2O_3 nanoparticles' thermal conductivity.

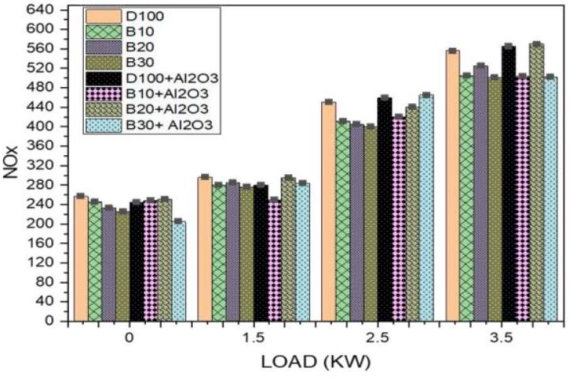

Figure 6 Graph for NOx versus loads.

3. Formation of Mathematical Model

We consider the following system of differential equations:

$$\begin{aligned}\frac{dG}{dt} &= Q + \frac{\lambda B}{1+\beta_1\beta NB} - \gamma_1 G\\ \frac{dB}{dt} &= rB\left(1-\frac{B}{K}\right) - \gamma_2 B\\ \frac{dN}{dt} &= A - \beta NB - \gamma N.\end{aligned} \tag{3.1}$$

Where $G(0) = G_0 > 0, B(0) = B_0 \geq 0, N(0) = N_0 > 0$.
In model system (3.1), $G(t)$, $B(t)$ and $N(t)$ be the density of emission of gasses from CI engines, biodiesel, and nanoparticles respectively. r and K are intrinsic growth rate and carrying capacity of biodiesel respectively. γ_2 represents the depletion rate of biodiesel through different factors such as accidents etc. In the above system (3.1), density of emission of gasses from CI engine is based on biodiesel with interaction term λ and emission of gasses become decrease through interaction term β_1 with nanoparticles. Q and γ_1 are constant density of gasses present in the environment and natural depletion of gasses respectively. A, β and γ are constant density of nanoparticles present in the environment, nanoparticle depletion through interaction between nanoparticle and biodiesel and natural depletion respectively.

Lemma: The region of attraction for the system (3.1) is given by the set:
$\Omega = \{(G, B, N) : 0 < G \leq G_m, 0 \leq B \leq B_m, 0 < N \leq N_m\}$
where

$$G_m = \frac{Q + \lambda B_m}{\gamma_1}, B_m = \frac{(r-\gamma_2)K}{r} \text{ and } N_m = \frac{A}{\gamma}$$

and it attracts all solutions initiating in the interior of the positive octant.

4. Equilibrium analysis

There exist only two equilibrium points $E_0\left(\frac{Q}{\gamma_1}, 0, \frac{A}{\gamma}\right)$ and $E_1(G^*, B^*, N^*)$. The equilibrium point $E_0\left(\frac{Q}{\gamma_1}, 0, \frac{A}{\gamma}\right)$ is always positive. Now, find the equilibrium point $E_1(G^*, B^*, N^*)$ as follows:
Existence of $E_1(G^*, B^*, N^*)$
Here G^*, B^* and N^* are the positive solutions of the following algebraic equations:

$$Q + \frac{\lambda B^*}{1+\beta_1\beta N^* B^*} - \gamma_1 G^* = 0 \tag{4.1}$$

$$rB^*\left(1-\frac{B^*}{K}\right) - \gamma_2 B^* = 0 \tag{4.2}$$

$$A - \beta N^* B^* - \gamma N^* = 0 \tag{4.3}$$

From equation (4.2), we get
$B^* = \frac{K(r-\gamma_2)}{r}$.
The value of B^* is always positive with condition
$r > \gamma_2$
After simple manipulation, we get from equation (4.3) is
$N^* = \frac{Ar}{\beta(r-\gamma_2)K+\gamma r}$.
Putting the value of B^* and N^* in equation (4.1), we get
$G^* = \frac{Q}{\gamma_1} + \frac{\lambda B^*}{\gamma_1\left[1+\beta_1(A-\gamma N^*)\right]}$.

5. Stability Analysis

5.1 Local Stability The entries of general variational matrix are given by differentiating the right side of system (3.1) with respect to G, B and N i.e.

$$V(E) = \begin{pmatrix} t_{11} & t_{12} & t_{13} \\ 0 & t_{22} & 0 \\ 0 & t_{32} & t_{33} \end{pmatrix}$$

Where $t_{11} = -\gamma_1, t_{12} = \frac{\lambda}{(1+\beta\beta_1 NB)^2}, t_{13} = -\frac{\lambda\beta\beta_1 B^2}{(1+\beta\beta_1 NB)^2}, t_{22} = r - \gamma_2 - \frac{2rB}{K}, t_{32} = -\beta N$, $t_{33} = -\beta B - \gamma$.

The variational matrix $V(E_0)$ at equilibrium point E_0 is given by

$$V(E_0) = \begin{pmatrix} -\gamma_1 & \lambda & 0 \\ 0 & r-\gamma_2 & 0 \\ 0 & -\frac{\beta A}{\gamma} & -\gamma \end{pmatrix}.$$

Since one eigenvalue corresponding to B - direction of matrix $V(E_0)$ is always positive with condition (4.5). So E_0 has unstable manifold in B-direction and stable manifold in $G - N$ plane.
The variational matrix $V(E_1)$ at equilibrium point E_1 is given by

$$V(E_1) = \begin{pmatrix} -\gamma_1 & a_{12} & a_{13} \\ 0 & -(r-\gamma_2) & 0 \\ 0 & -\beta N^* & -\beta B^* - \gamma \end{pmatrix}.$$

Where $a_{12} = \frac{\lambda}{(1+\beta\beta_1 N^* B^*)^2}, a_{13} = -\frac{\lambda\beta\beta_1 B^{*2}}{(1+\beta\beta_1 N^* B^*)^2}$.

From variational matrix, all three eigen values are negative in $G-$ direction, B - direction and $N-$ direction respectively. So, the system is stable in $G - B - N-$ plane.

5.2 Global Stability In this section, we consider the global stability of system (3.1) by constructing a suitable Lyapunov function.

Theorem (5.2.1): Let the following inequality holds
$\beta^2 N^{*2} < \frac{r\gamma}{K}, \lambda^2 < \min\left\{\frac{\gamma_1 r}{K}, \frac{\gamma_1\gamma(1+\beta\beta_1 N^* B^*)^2}{\beta^2\beta_1^2 B^{*4}}\right\}$.
Then system (3.1) is globally asymptotically stable in the interior of positive octant Ω.

Proof:

For global stability, we consider positive definite function $H(G, B, N)$ as
$H = \frac{1}{2}(G - G^*)^2 + \frac{1}{2}(N - N^*)^2 + B - B^* - B^* \ln \frac{B}{B^*}$.
Differentiating V with respect to time t along the solution of system (5.2.1), we get
$\frac{dH}{dt} = (G - G^*)\frac{dG}{dt} + (N - N^*)\frac{dN}{dt} + \frac{(B-B^*)}{B}\frac{dB}{dt}$.
Using equation giving interior equilibrium point E_1 and after some algebraic manipulations, we have

$$\frac{dH}{dt} = -\gamma_1 (G - G^*)^2 - \frac{r}{K}(B - B^*)^2 - (\gamma + \beta B)(N - N^*)^2 - \beta N^* (B - B^*)(N - N^*) + \frac{\lambda}{(1 + \beta\beta_1 NB)}\left[1 - \frac{N\beta\beta_1 B^*}{(1 + \beta\beta_1 N^* B^*)}\right](B - B^*)(G - G^*) - \frac{\lambda\beta\beta_1 B^{*2}}{(1 + \beta\beta_1 NB)(1 + \beta\beta_1 N^* B^*)}(N - N^*)(G - G^*).$$

We note that $\dot{H}$ can be made negative definite inside Ω if
$\beta^2 N^{*2} < \frac{r\gamma}{K}, \lambda^2 < \min\left\{\frac{\gamma_1 r}{K}, \frac{\gamma_1\gamma(1+\beta\beta_1 N^* B^*)^2}{\beta^2\beta_1^2 B^{*4}}\right\}$.
Hence H is a Lyapunov function with respect to E_1 and positive equilibrium point E_1 is globally asymptotically stable with respect to all solutions initiating in the interior of the positive octant Ω. This completes the proof of the theorem (5.2.1).

6. Numerical Simulation

To facilitate the interpretation of our mathematical findings by numerical simulation, we solve the system (3.1) using fourth order Runge-kutta method under the following set of compatible parameters with the help of MATLAB Software package.

Consider the following set of parameter values to study system (3.1), numerically. $Q = 5, \lambda = 0.08, \beta = 0.01, \beta_1 = 0.01, \gamma_1 = 0.18, r = 0.2, K = 100, \gamma_2 = 0.02, A = 20, \gamma = 0.02$.

For the above set of parameter values, interior equilibrium point is given by $E_1(61.2323, 90, 21.7391)$

The characteristic equation corresponding to the variational matrix $V(E_1)$ is given by $\lambda^3 + 1.28\lambda^2 + 0.3636\lambda + 0.029808 = 0$.

The eigenvalues of above characteristic equation are $-0.92, -0.18, -0.18$. Since eigenvalues have negative real parts, which show that equilibrium point E_1 is locally asymptotically stable.

Figures have been plotted between dependent variables and time for different parameter values to shows changes occurring in population with time under different conditions. The results of numerical simulation are displayed graphically. From figure (7), it is noted for given initial values the population tend to their corresponding value of equilibrium point E_1 and hence exists in the form of steady state assuring local stability of E_1. We can easily see from figure (8), equilibrium point E_1 is globally

asymptotically stable. Global stability shows that all solutions initiating in the interior of the positive octant settle down to their respective equilibrium level for larger time. From figure 9, we can conclude, when nanoparticle added in the biodiesel then gas emission from CI engine decreases. That means increases the value of β, the density of the gas emission decreases. Figure 10 represents the surface plot of the system.

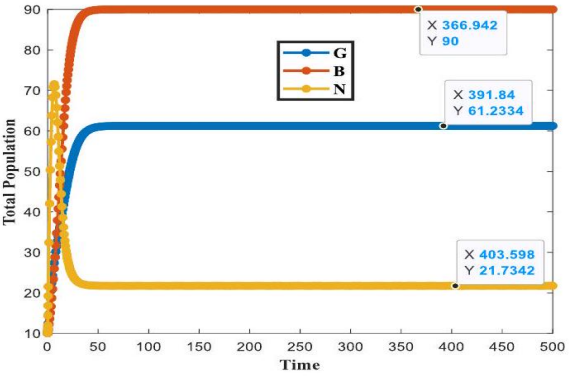

Figure: 7 Stable behaviour of $\boldsymbol{G}, \boldsymbol{B}$ and $\boldsymbol{N}$ with time and other parameter values are same (6.1).

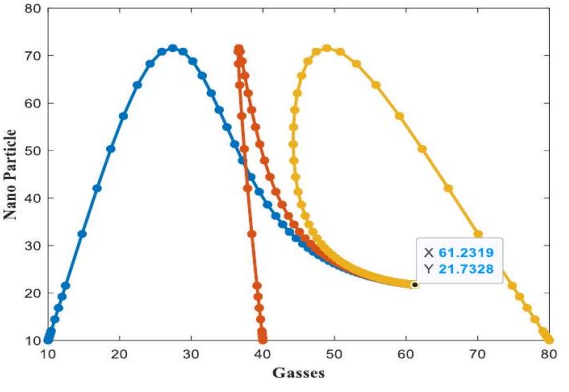

Figure: 8 Global Stability behaviour of the system

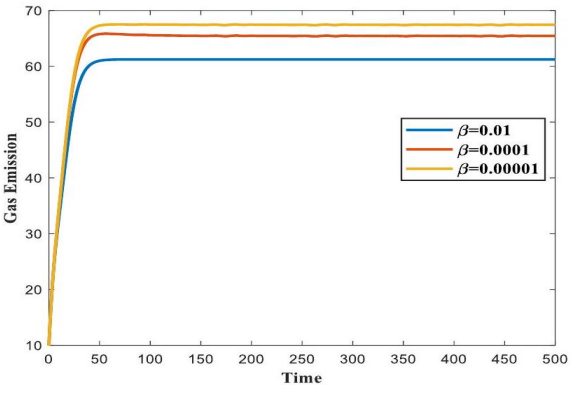

Figure: 9 Variation of Gas Emission from CI Engine with time for different values of β.

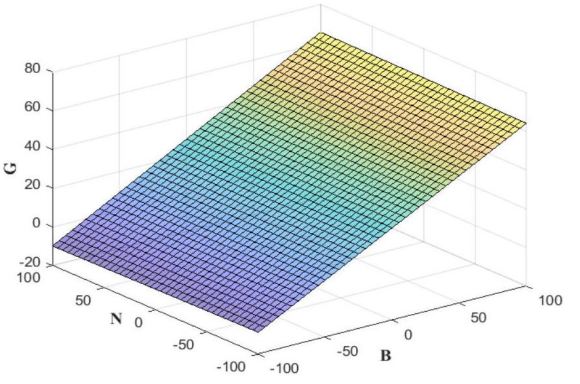

Figure: 10 Surface plot of the system.

7. Conclusion

In this paper, a nonlinear mathematical model is proposed and analysed to see the effect of adding nanoparticle in the biodiesel. We also used experimental data to compare our analytical results. From experimentally, we find, Alumina nanoparticles were used with rice bran biofuel to provide extremely significant performance and emission outcomes. The characteristics of aluminium oxide nanoparticles and the widespread availability of rice bran made the amount of sulphur in the exhaust emissions insignificant. The experiment's sequence of actions and the results that resulted from them are summed up as follows:

- At 0 kW, 1.5 kW, 2.5 kW, and 3.5 kW , respectively, the NO_x content dropped by 18.19%, 13.34%, 12.20%, and 8.89% for RB30A190, RB10A190, RB30, and RB30.

- The largest CO2 emission decrease of 8.6% was observed for B20 biofuel at 0 kW load and 3.82% for B10 fuel at 1.5 kW load; however, at 2.5 kW load, the CO 2 content of RB10 was equivalent to that of plain diesel.
- Compared to clean diesel (D100), the impact of Al_2O_3 nanoparticles and the use of rice bran biofuel mixed fuel on engine performance was noted. For example, BSFC increased by 40% for RB20Al30 at 3.5 kW load, and BTE increased by 9.67% for RB30 at 1.5 kW load.
- The main finding of this experimental investigation is that alumina nanoparticles combined with rice bran BD are a highly efficient way to improve performance and manage pollution. The fuel's combustion characteristics were impacted by the Al_2O_3 nano additions. It is necessary to conduct more study on some injection timing adjustments for CI engines.

Acknowledgement

The Maharishi University of Information Technology, Lucknow, the Institute of Engineering and Technology, Lucknow, and the Faculty of Engineering and Technology, University of Lucknow, are all deeply appreciated by the authors for their help during this research.

Author contributions:

Conceptualisation: Abhijeet Maurya, Bhanu Pratap Singh,Ajay Kumar Sharma ; *Software:* Rachana Pathak ; *Writing-Original Draft:* Abhijeet Maurya, Bhanu Pratap Singh,Ajay Kumar Sharma, Rachana Pathak

Conflicts of Interest: The authors declare no conflict of interest.

References

[1] A.I. EL-Seesy, Z. He, H. Hassan, D. Balasubramanian, Improvement of combustion and emission characteristics of a diesel engine working with diesel/jojoba oil blends and butanol additive, Fuel.279(2020)118433. https://doi.org/10.1016/J.FUEL.2020.118433.

[2] A.I. EL-Seesy, T. Xuan, Z. He, H. Hassan, Enhancement the combustion aspects of a CI engine working with Jatropha biodiesel/decanol/propanol ternary combinations, Energy Conversion and Management. 226 (2020) 113524. https://doi.org/10.1016/J.ENCONMAN.2020.113524

[3] A.I. EL-Seesy, H. Hassan, Investigation of the effect of adding graphene oxide, graphene nanoplatelet, and multiwalled carbon nanotube additives with n-butanolJatropha methyl ester on a diesel engine performance, Renewable Energy.132(2019)558-574. https://doi.org/10.1016/J.RENENE.2018.08.026.

[4] A.Prabu, Nanoparticles as additive in biodiesel on the working characteristics of a DI diesel engine, Ain Shams Engineering Journal. 9(2018)2343-2349. https://doi.org/10.1016/J.ASEJ.2017.04.004.

[5] M.F. Al-Dawody, M.S. Edam, Experimental and numerical investigation of adding castor methyl ester and alumina nanoparticles on performance and emissions of a diesel engine, Fuel.307(2022). https://doi.org/10.1016/j.fuel.2021.121784.

[6] M.E.M. Soudagar, N.N. Nik-Ghazali, M. Abul Kalam, I.A. Badruddin, N.R. Banapurmath, N. Akram, The effect of nano-additives in diesel-biodiesel fuel blends: A comprehensive review on stability, engine performance and emission characteristics, Energy Conversion and Management. 178(2018)146-177. https://doi.org/10.1016/J.ENCONMAN.2018.10.019.

[7] V. Saxena, N. Kumar, V.K. Saxena, A comprehensive review on combustion and stability aspects of metal nanoparticles and its additive effect on diesel and biodiesel fuelled C.I. engine, Renewable and Sustainable Energy Reviews.70(2017)563-588. https://doi.org/10.1016/j.rser.2016.11.067.

[8] A.E. Elwardany, M.N. Marei, Y. Eldrainy, R.M. Ali, M. Ismail, M.M. El-kassaby, Improving performance and emissions characteristics of compression ignition engine: Effect of ferrocene nanoparticles to diesel-biodiesel blend, Fuel.270(2020). https://doi.org/10.1016/j.fuel.2020.117574.

[9] A.I. El-Seesy, A.M.A. Attia, H.M. El-Batsh, The effect of Aluminium oxide nanoparticles addition with Jojoba methyl ester-diesel fuel blend on a diesel engine performance, combustion and emission characteristics, Fuel.224(2018)147-166. https://doi.org/10.1016/j.fuel.2018.03.076.

[10] M.I. Al-Widyan, M.A. Al-Muhtaseb, Experimental investigation of jojoba as a renewable energy source, Energy Conversion and Management.51(2010)1702-1707. https://doi.org/10.1016/J.ENCONMAN.2009.11.043.

[11] M.S. Shehata, S.M.A. Razek, Experimental investigation of diesel engine performance and emission characteristics using jojoba/diesel blend and sunflower oil, Fuel.90(2011)886-897. https://doi.org/10.1016/J.FUEL.2010.09.011.

[12] A.T. Hoang, M. Tabatabaei, M. Aghbashlo, A.P. Carlucci, A.I. Ölçer, A.T. Le, A. Ghassemi, Rice bran oil-based biodiesel as a promising renewable fuel alternative to Petro diesel: A review, Renewable and Sustainable EnergyReviews.135(2021). https://doi.org/10.1016/j.rser.2020.110204.

[13] C.S. Aalam, C.G. Saravanan, Effects of nano metal oxide blended Mahua biodiesel on CRDI diesel engine, Ain Shams Engineering Journal.8(2017)689-696. https://doi.org/10.1016/J.ASEJ.2015.09.013.

[14] J. Sadhik Basha, R.B. Anand, Role of nanoadditive blended biodiesel emulsion fuel on the working characteristics of a diesel engine, Journal of Renewable and Sustainable Energy.3(2011)023106. https://doi.org/10.1063/1.3575169.

[15] S.H. Hosseini, A. Taghizadeh-Alisaraei, B. Ghobadian, A. Abbaszadeh-Mayvan, Effect of added alumina as nano-catalyst to diesel-biodiesel blends on performance and emission characteristics of CI engine, Energy. 124 (2017) 543-552. https://doi.org/10.1016/j.energy.2017.02.109.

[16] M.A. Fayad, H.A. Dhahad, Effects of adding aluminium oxide nanoparticles to butanoldiesel blends on performance, particulate matter, and emission characteristics of diesel engine, Fuel. 286(2021). https://doi.org/10.1016/j.fuel.2020.119363.

[17] S. Sinha, A.K. Agarwal, S. Garg, Biodiesel development from rice bran oil: Transesterification process optimization and fuel characterization, Energy Conversion and Management.49(2008)1248-1257.

[18] S. Vellaiyan, K.S. Amirthagadeswaran, Zinc oxide incorporated water-in-diesel emulsion fuel: Formulation, particle size measurement, and emission characteristics assessment, https://doi.org/10.1080/10916466.2015.1122621.

[19] Pj. Prakash, Gr. Reddy, Bs. Rao,Performance of DI Diesel Engine with Rice Bran Biodiesel and Al 203 Nano Additive, International Journal of Engineering Research in Mechanical and Civil Engineering (IJERMCE). 2 (2017) 2456-1290.

[20] Ali Aghababai Beni and Hadi Jabbari, (2022), Nanomaterials for Environmental Applications, Results in Engineering, 15(2022), 100467.

[21] G. Suganya and R. Senthamarai, (2022), Mathematical modeling and analysis of Phytoplankton-Zooplankton-Nanoparticle dynamics, 9(2), 333-341.

Abhijeet Maurya, Maharishi University of Information Technology, Lucknow, Uttar Pradesh, India
e-mail: abhijeetmaurya007@gmail.com, *corresponding Author

Bhanu Pratap Singh, Maharishi University of Information Technology, Lucknow, Uttar Pradesh, India

Ajay Kumar Sharma, Institute of Engineering & Technology, AKTU, Lucknow Uttar Pradesh

Rachana Pathak, Department of Applied Science and Humanities (Mathematics), Faculty of Engineering and Technology, University of Lucknow, Lucknow, Uttar Pradesh, India
e-mail: rachanapathak2@gmail.com